The Astrophysical Journal, 937:123 (13pp), 2022 October 1 https://doi.org/10.3847/1538-4357/ac8eb4

Origin of Nitrogen Isotopic Variations in the Rocky Bodies of the Solar System

Damanveer S. Grewal
Division of Geological and Planetary Sciences, California Institute of Technology, 1200 E California Blvd, Pasadena, CA 91125, USA; dgrewal@caltech.edu
Received 2022 May 16; revised 2022 August 25; accepted 2022 August 27; published 2022 October 5

Abstract

Noncarbonaceous (NC; inner solar system) meteorites have lower $^{15}N/^{14}N$ ratios than carbonaceous (CC; outer solar system) meteorites. Whether this is evidence of a primordial heterogeneity of N reservoirs in the protosolar disk remains unclear. In this study, I consider the N isotopic compositions of meteorite (chondrite, achondrite, and iron meteorite) parent bodies as a function of their growth zones. Despite the $^{15}N/^{14}N$ ratios of CC meteorites being generally higher than NC meteorites, there is a substantial overlap between them. Late-stage mixing of isotopically distinct reservoirs cannot explain this overlap. $^{15}N/^{14}N$ ratios of meteorites, independent of the growth zones, are correlated with the accretion ages of their parent bodies. A common correlation of the $^{15}N/^{14}N$ ratios of NC and CC chondrites with their peak metamorphic temperatures suggests that N isotopic compositions of meteorites were likely set by a universal time-dependent process—thermal evolution of their parent bodies by radiogenic heating. Therefore, heterogeneous N isotopic compositions of meteorites do not allude to isotopically heterogeneous primitive N reservoirs in the protosolar disk. Rather, it is likely that the N isotopic compositions of meteorites are a direct reflection of a differential response of labile ^{15}N-rich and refractory ^{15}N-poor components in common organic precursors to variable degrees of parent body processing. Consequently, the isotopic ratios of N, and other highly volatile elements like C and H, in meteorites do not reflect the isotopic compositions of primitive volatile reservoirs in the protosolar disk and thus cannot be used independently to cosmolocate volatile reservoirs in the disk.

Unified Astronomy Thesaurus concepts: Meteorites (1038); Iron meteorites (863); Chondrites (228); Planetesimals (1259); Protoplanetary disks (1300); Planet formation (1241)

1. Introduction

Unraveling the origin of nitrogen (N) and other life-essential volatiles like carbon (C) and water (H_2O) in rocky bodies is key to understanding the formation of habitable worlds in our solar system and beyond. The isotopic compositions of these volatiles in terrestrial and extraterrestrial samples have been used to track their journey from primordial gas and solids to the first formed planetesimals and finally to the fully formed rocky planets in the solar system (Alexander et al. 2012; Marty 2012; Füri & Marty 2015; Dasgupta & Grewal 2019; Grewal et al. 2021b). The large variation of $^{15}N/^{14}N$ ratios in extraterrestrial samples makes it a crucial proxy in identifying the relationship between the volatile inventories of different cosmochemical reservoirs (Marty 2012; Füri & Marty 2015). Although the $^{15}N/^{14}N$ ratios of bulk meteorites (relics of early forming planetesimals) show substantial inter- and intra-group variation, they are distinctly higher and lower than those of the protosolar nebular gas (PSN) and cometary reservoirs, respectively (Figure 1; N isotopic composition is generally expressed as $\delta^{15}N\ (‰) = [(^{15}N/^{14}N)_{sample}/(^{15}N/^{14}N)_{atm}–1] \times 1000$ where $(^{15}N/^{14}N)_{atm}$ is the ratio of N isotopes in the Earth's atmosphere (3.676×10^{-3}) (Marty et al. 2011; Marty 2012). Importantly, $^{15}N/^{14}N$ ratios of the bulk silicate Earth (BSE = mantle + crust + exosphere) and Martian interior lie within the range of different types of meteorites (Mathew & Marti 2001; Alexander et al. 2012). This observation suggests that the parent bodies of meteorites and rocky planets acquired their N from a common reservoir that was isotopically distinct from the PSN and cometary reservoirs.

The growth zones and accretion ages (defined relative to the formation of calcium-aluminum-rich inclusions (CAIs)—oldest solids that date *time zero* of solar system formation and treated as instantaneous events in this study) of the parent bodies of meteorites in the protosolar disk are now reasonably constrained due to the recent advances in isotope cosmochemistry. Nucleosynthetic anomalies of Ti, Cr, and Mo in meteorites reveal a fundamental isotopic dichotomy, i.e., the parent bodies of meteorites derived from two isotopically distinct reservoirs, noncarbonaceous (NC) and carbonaceous (CC) (Warren 2011; Kleine et al. 2020). These reservoirs were isolated from each other for the first few million years after the formation of CAIs (Kruijer et al. 2017). NC and CC meteorites most likely are representative of inner and outer solar system materials, respectively (Kruijer et al. 2017; Kleine et al. 2020). Primitive meteorites (known as chondrites) belonging to the CC reservoir (e.g., CI, CM, and CR chondrites) are enriched in N, C, and H_2O (Pearson et al. 2006; Alexander et al. 2012). The rough similarity of their $^{15}N/^{14}N$ and D/H ratios with those of the BSE makes planetesimals sourcing the CC reservoir the primary source of volatiles in the Earth and other rocky bodies in the inner solar system (e.g., Alexander et al. 2012; Marty 2012). However, alternate evidence suggests that inner solar system planetesimals did not necessarily accrete N-, C-, and H_2O-free materials, thereby relaxing the constraint for an exclusively outer solar system origin of volatiles in the inner solar system protoplanets and planets. The $^{15}N/^{14}N$ and D/H ratios of Earth's primitive mantle are similar to those of enstatite chondrites (ECs; primitive meteorites belonging to the NC reservoir, which are isotopically similar to inner solar system planets in multi-isotope space) (Javoy 1997; Piani et al. 2020). This suggests that N-, C-, and H_2O-bearing materials were not only locally accreted by the inner solar system

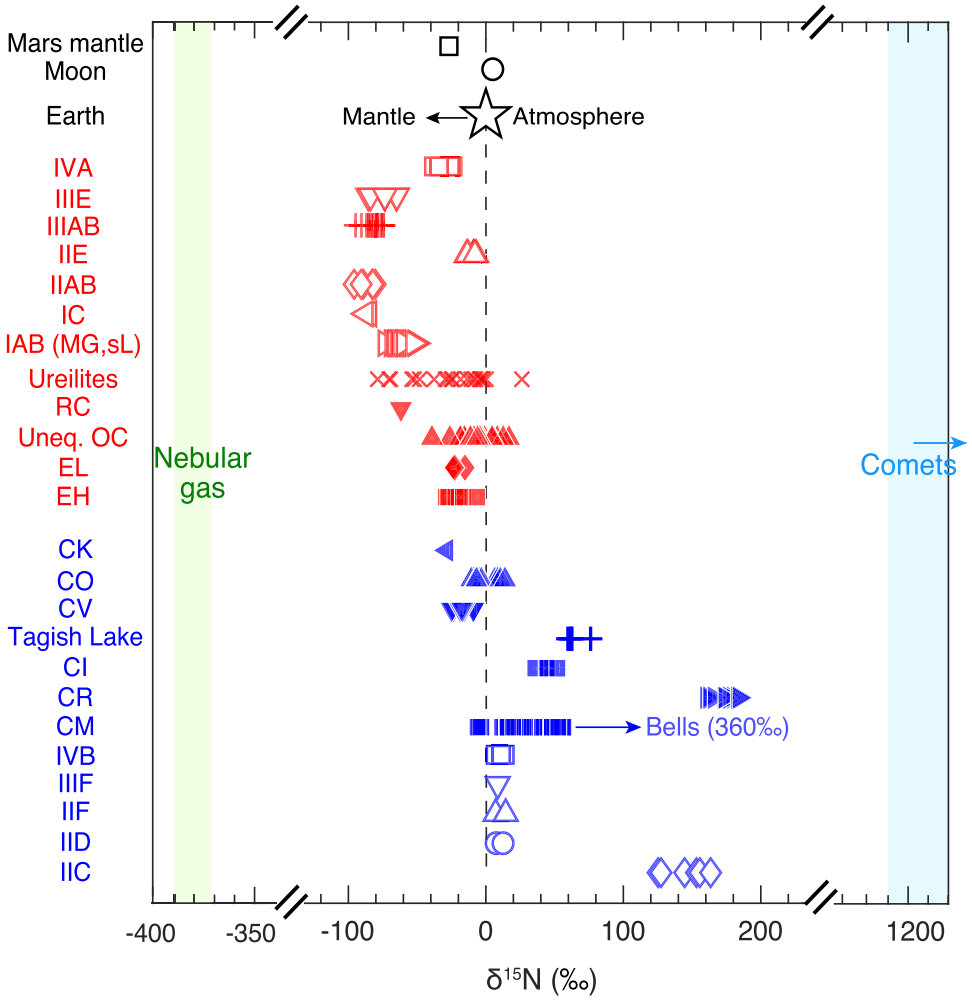

Figure 1. Nitrogen isotopic compositions of cosmochemical reservoirs in the solar system. δ^{15}N values of bulk meteorites (chondrites, ureilites, and iron meteorites), Earth's mantle and atmosphere, Moon and Martian mantle are distinct relative to the ^{15}N-poor PSN and ^{15}N-rich cometary reservoirs. Meteorites are plotted in red and blue using the NC-CC classification based on the isotopic anomalies of Cr, Ti, and Mo. Refer to Table A1 in the Appendix and the compilation of Grewal et al. (2021b) for the source of the data for the δ^{15}N values.

planetesimals within ~2 Ma after the formation of CAIs (based on the estimated accretion age of the EC parent body Sugiura & Fujiya 2014) but also contributed substantially to the volatile budgets of present-day rocky planets. Recently, it has been shown that the N isotopic compositions of iron meteorites (remnants of the cores of earliest formed protoplanets in the solar system) mirror the NC-CC dichotomy with NC irons having distinctly lower ^{15}N/^{14}N ratios than CC irons (Grewal et al. 2021b). The observation is in general agreement with the reported increase in ^{15}N/^{14}N ratios in solar system reservoirs with increasing heliocentric distance (Füri & Marty 2015). As the parent bodies of some NC iron meteorites accreted as early as ~0.1 Ma after CAIs (Kruijer et al. 2017), an NC-CC dichotomy of N isotopes in iron meteorites suggests that planetesimals in the inner disk were not only accreting N-bearing materials from the very beginning, but also their N was sourced from a reservoir that was isotopically distinct to the outer solar system (Grewal et al. 2021b).

The cause behind the large N isotopic variations between NC and CC meteorites, however, remains unclear. Does it reflect a spatial heterogeneity in the N isotopic compositions of nebular solids? Almost the entire N and C, and a substantial H, inventory of primitive chondrites is hosted in organic matter (Alexander et al. 1998, 2017). For the above scenario to be valid, organics in the NC reservoir must have had lower ^{15}N/^{14}N ratios than in the CC reservoir. This could be due to either selective destruction of ^{15}N-rich components via nebular processing in the inner disk or higher production of ^{15}N-rich components in the outer disk (in the case of a presolar or an outer solar system origin of organics, respectively), resulting in higher ^{15}N/^{14}N ratios of CC planetesimals (Grewal et al. 2021b). If N isotopic compositions of the starting materials are directly reflected in the measured values of meteorites, a primordial N isotopic heterogeneity in the meteorite record necessitates an ineffective role of parent body processing (i.e., thermal metamorphism and aqueous alteration) in altering the ^{15}N/^{14}N ratios. Or, if parent body processing was effective, its impact was almost identical in the parent bodies of both NC and CC meteorites such that the relative differences between the ^{15}N/^{14}N ratios of primitive NC and CC organics are reflected in present-day meteorites. Alternately, planetesimals in both NC and CC reservoirs could have inherited isotopically and chemically similar organics and the unique ^{15}N/^{14}N ratios recorded by the meteorites are a direct reflection of the effects of parent body processing. Organic matter in chondrites could have been affected by parent body processing as its

components exhibit differential stabilities to thermal metamorphism and aqueous alteration (Alexander et al. 1998; Sephton et al. 2003; Alexander et al. 2007; Foustoukos et al. 2021). A differing response of these components to the nature and extent of parent body processing could result in the variability of N isotopic compositions exhibited by meteoritic samples. In this case, the lower and higher $^{15}N/^{14}N$ ratios of NC and CC meteorites simply reflect the effects of differential parent body processing on common organic progenitors.

If the first scenario is true, then the NC–CC dichotomy of N isotopic compositions observed in iron meteorites truly reflects the presence of starting materials with distinct $^{15}N/^{14}N$ ratios in the inner and outer regions of the protosolar disk. If the second scenario is valid, then the bimodal distribution of N isotopes is related not to the heterogeneous distribution of N carriers but to the variable effects of parent body processing in planetesimals. The relationship between the N isotopic compositions of meteorites and the BSE is also important to constrain the contribution of inner and outer solar system materials to the N budget of the Earth and consequently the dynamics of planetary growth. It is therefore critical to examine whether the $^{15}N/^{14}N$ ratios of meteorites directly reflect the N isotopic compositions of primitive volatile reservoirs in the disk or not. To answer these questions, I use the literature data to track the spatial and temporal distribution of the $^{15}N/^{14}N$ ratios of all classes of meteorites (chondrites, achondrites, and iron meteorites) and assess the effects of parent body processing on the N isotopic compositions of planetesimals.

2. Nitrogen Isotopic Compositions of Planetesimals in the Inner and Outer Protosolar Disk

The existence of only two stable isotopes rules out using a *three-isotope plot* to accurately infer the cosmochemical history of N. Comparing $^{15}N/^{14}N$ ratios with mass-independent isotopic signatures of elements like Ti, Cr, and Mo in meteorites provides an alternate path to track the N isotopic compositions of planetesimals as a function of their growth zones. Grewal et al. (2021b) used this approach with iron meteorites to infer the N isotopic compositions of the earliest formed protoplanets in the inner and outer disk. While parent bodies of iron meteorites formed within ~1 Ma after CAIs (Kruijer et al. 2014), the accretion ages of several groups of chondrites and achondrites attest that planetesimals continued to accrete for ~3–4 Myr after CAIs (Sugiura & Fujiya 2014). Further, the N inventory of iron meteorites—incorporated into the alloy melts during core-mantle differentiation (Grewal et al. 2021b)—is biased toward its abundances and isotopic ratios in planetesimal interiors at the tail-end of their thermal evolution. Therefore, to develop a comprehensive understanding of the spatial and temporal distribution of the N isotopic compositions of planetesimals in the solar system, it is imperative to investigate the entire meteorite record—chondrites, achondrites, and iron meteorites.

Chondrites (enstatite (ECs), Rumuriti (RCs), ordinary (OCs), and carbonaceous (CCs)) are primitive meteorites that accreted ~2–4 Ma after CAIs (Sugiura & Fujiya 2014). ECs, RCs, and OCs sample inner solar system planetesimals whereas CCs sample outer solar system ones (Warren 2011). Their undifferentiated character makes chondrites—originating from surficial to sub-surficial layers—the best analogs of the primitive materials accreted by rocky bodies (Alexander et al. 2007, 2012). In contrast to iron meteorites, where most of the N is dissolved in crystallized Fe, Ni-alloy phases (kamacite and taenite; Prombo & Clayton 1993), chondrites host almost all their N in organic matter (except ECs where the identity of the primitive N hosts is completely masked by thermal metamorphism under extremely reduced conditions) (Alexander et al. 1998; Sephton et al. 2003; Alexander et al. 2007). Stony achondrites are basaltic or plutonic rocks reprocessed to varying degrees by melting and recrystallization within their parent bodies (Keil 2010, 2012). They are either products (differentiated achondrites like angrites, aubrites, and HEDs) or residues (primitive achondrites like acapulcoites, brachinites, lodranites, ureilites, and winonaites) of partial melting, containing N either in the form of dissolved N_2, or bonded NH_4^+/N^{3-} in the silicate network (Grady et al. 1986; Abernethy et al. 2018). However, N abundances and isotopic compositions of angrites, aubrites, and HEDs (basaltic rocks or cumulates sampling the crustal to sub-crustal reservoirs) are severely affected by volatile loss during secondary processes like basaltic volcanism and associated degassing (Abernethy et al. 2013), ruling out their utility. Further, there exists little to no data for the N isotopic compositions of acapulcoites, brachinites, lodranites, and winonaites. N isotopic compositions of pallasites—stony-iron meteorites composed of olivine crystals in a Fe, Ni-matrix originating from either the core-mantle boundary or impact-induced mixtures of differentiated planetesimals—are also known to be affected by N loss following Rayleigh distillation (Franchi et al. 1993). Ureilites—ultramafic achondrites representing the mantle residues of their parent bodies—are the only group of stony achondrites whose N isotopic compositions are extensively reported and have not undergone significant mass-dependent isotopic fractionation during degassing (e.g., Grady et al. 1985; Rai et al. 2003). Hence, in this study, I have used the $^{15}N/^{14}N$ ratios of chondrites, iron meteorites, and ureilites to infer the N isotopic compositions of planetesimals in the inner and outer protosolar disk. $\delta^{15}N$ values of individual samples of chondrites and ureilites are reported in Table A1 in the Appendix. The data compilation of Grewal et al. (2021b) is used for the $\delta^{15}N$ values of iron meteorites.

To track the N isotopic compositions of planetesimals as a function of their growth zones, I plotted the $\delta^{15}N$ values of meteorites against the mass-independent anomalies of Cr, Ti, and Mo (elements instrumental in identifying the NC-CC dichotomy) (Figure 2). Averaged $\delta^{15}N$ values of all meteorite groups are reported in Table 1. Agreeing with the observations of Grewal et al. (2021b), NC meteorites generally have lower $\delta^{15}N$ values than their CC counterparts. Mean $\delta^{15}N$ values of all NC meteorite groups lie between –86.9‰ and –4.1‰. The lower end of this range is defined by $\delta^{15}N$ values of IAB-MG, IC, IIAB, IIIAB, and IIIE irons (–86.9‰ to –60.6‰). $\delta^{15}N$ values of other NC irons (IVA and IIE) are substantially higher ($-28.9‰ \pm 5.2‰$ and $-4.1‰ \pm 2.7‰$, respectively). $\delta^{15}N$ values of NC chondrites, i.e., ECs ($-21.0‰ \pm 6.2‰$), OCs ($-6.6‰ \pm 12.1‰$; excluding the two anomalous OCs reported in Sugiura & Hashizume 1992), and RCs (–61.8‰), along with ureilites ($-23.7‰ \pm 26.0‰$; excluding the extensively weathered North Haig sample reported in Grady et al. 1985), lie within the range of inner solar system reservoir as defined by NC irons. In agreement with the observations of Grewal et al. (2021b) for NC irons, the mean $\delta^{15}N$ values of all NC chondrites and achondrites are less than 0‰. Mean $\delta^{15}N$ values of all groups of CC meteorites (except CB and CH) lie between –28.4‰ and 175.7‰. The $\delta^{15}N$ values for the lower end are

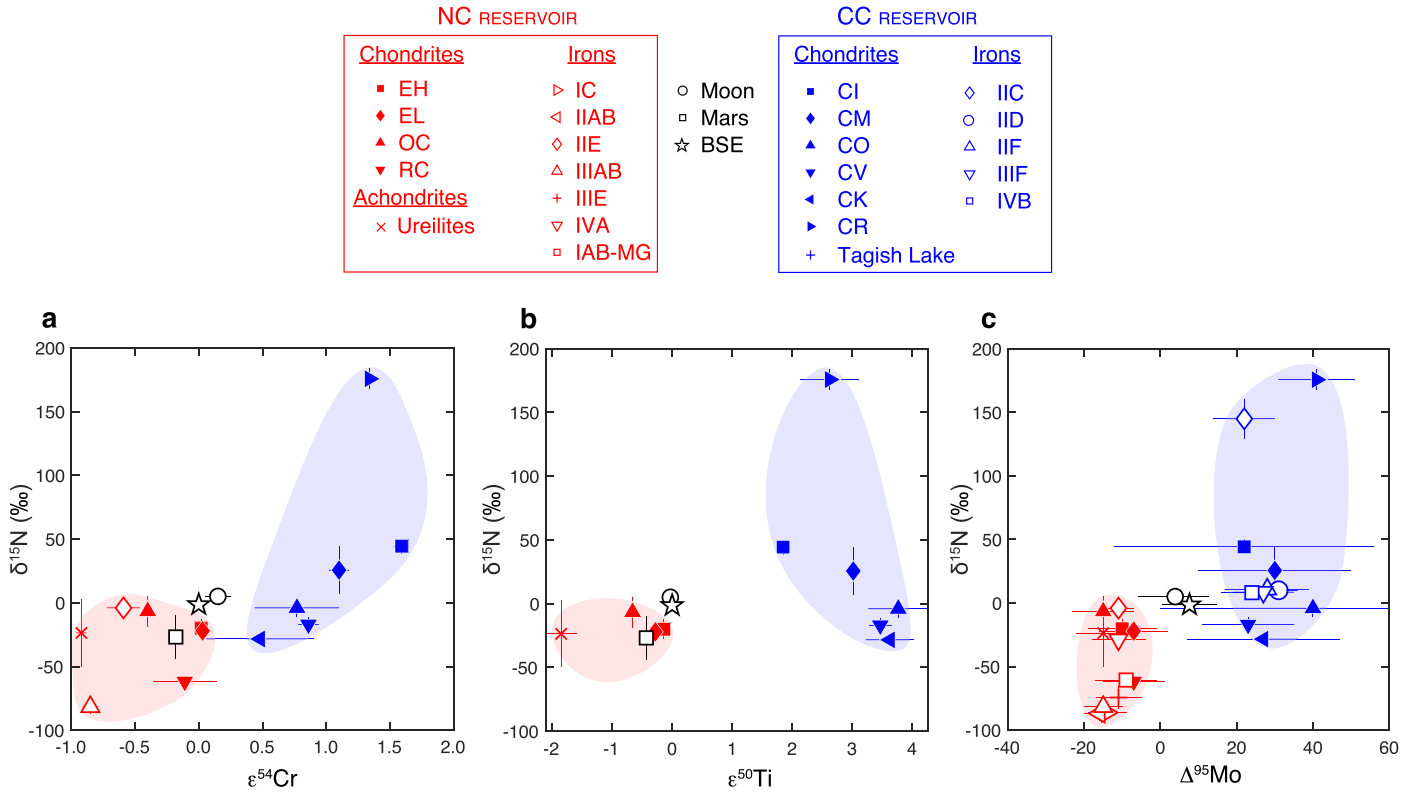

Figure 2. Isotopic compositions of the rocky bodies from NC and CC reservoirs plotted in δ^{15}N–ε^{54}Cr, δ^{15}N–ε^{50}Ti, and δ^{15}N–Δ^{95}Mo space. Even though δ^{15}N values of NC meteorites (red) are generally lower than CC meteorites (blue), unlike ε^{54}Cr, ε^{50}Ti, and Δ^{95}Mo values, there is an overlap between the δ^{15}N values of NC and CC meteorites. δ and ε are the measure of isotopic ratios in parts per 1000 and 10,000, respectively. Δ^{95}Mo (=[ε^{95}Mo—0.596 × ε^{94}Mo] × 100) is the vertical deviation from the s-process mixing line (Budde et al. 2019). Error bars for ε^{54}Cr, ε^{50}Ti, and Δ^{95}Mo values are 2σ of the mean of the measurements, whereas for δ^{15}N values error bars are 1σ of the mean of the measurements. If absent, error bars are smaller than the symbol size. δ^{15}N values of meteorites are tabulated in Table 1. Data for the ε^{54}Cr, ε^{50}Ti, and Δ^{95}Mo values is compiled from Spitzer et al. (2020).

defined by CO (–4.1‰ ± 7.0‰), CV (–17.0‰ ± 5.9‰), and CK (–28.4‰ ± 1.6‰) groups, while the upper end is defined by CRs (175.7‰ ± 8.1‰) and IIC irons (144.9‰ ± 15.6‰). Mean δ^{15}N values of other CC iron groups (IID, IIF, IIIF, and IVB) lie between 8.1‰ and 10.8‰, whereas those of other CC chondrites, i.e., CI, CM (except Bells), and Tagish Lake are 44.3‰ ± 5.7‰, 25.6‰ ± 18.7‰, and 65.0‰ ± 6.6‰, respectively. Even though its O isotopic composition is similar to other CM chondrites, Bells is an anomalous CM chondrite with distinct chemical and isotopic compositions of several elements (Mittlefehldt 2002). It exhibits ^{15}N enrichments (δ^{15}N = 356.3‰ ± 4.9‰) analogous to CR chondrites (Alexander et al. 2007). δ^{15}N values of volatile-depleted, metal-rich CB (948‰ ± 35‰) and CH (858‰) chondrites are substantially higher than all other CC meteorites. However, unlike other CC chondrites, CB and CH chondrites do not contain a true matrix and their parent bodies formed rather late by the accretion from a gas-mantle plume generated by collisions between planetary embryos (Krot et al. 2009). Therefore, it is uncertain whether the δ^{15}N values of these rare chondrites represent the primitive N isotopic compositions of CC planetesimals and are hence not discussed in this study.

Unlike iron meteorites which showed a clear N isotopic dichotomy between NC and CC reservoirs (δ^{15}N values of NC and CC iron meteorites being lesser and greater than 0‰, respectively) (Grewal et al. 2021b), Figure 2 shows that there is an overlap between the N isotopic compositions of NC and CC reservoirs. δ^{15}N values of all CK, CO, and CV chondrites as well as some CM chondrites are less than 0‰. Also, δ^{15}N values of a few unequilibrated OCs and ureilites are greater than 0‰. This shows that unlike nonvolatile elements such as Cr, Ti, Mo, etc., N isotopic compositions do not exhibit a sharp boundary between the NC and CC planetesimals. This observation has important implications for the N isotopic compositions of primitive materials in the NC and CC reservoirs. Either (1) N-bearing materials in the inner and outer disk were indeed isotopically distinct resulting in an early NC-CC dichotomy of N isotopes (as sampled by NC and CC irons) and a late-stage mixing of materials between the two reservoirs is captured by the N isotopic compositions of some meteorites. For instance, if the N isotopic compositions of CO, CV, and CK chondrites (CC chondrites whose mean δ^{15}N values overlap with NC meteorites) reflect late-stage mixing of NC and CC reservoir, then their accretion ages must be younger than those of other CC chondrites. Or, (2) there was no true dichotomy between the N isotopic compositions of NC and CC reservoirs and the variable δ^{15}N values observed in corresponding meteorites is likely a result of the variability in parent body processing. To test the feasibility of these possibilities, I track the N isotopic compositions of the parent bodies of meteorites as a function of their accretion ages.

3. Nitrogen Isotopic Compositions of Planetesimals as a Function of Their Accretion Ages

A combination of ^{182}Hf–^{182}W ages and thermal models based on ^{26}Al decay are used to constrain the accretion ages of the parent bodies of iron meteorites (Kruijer et al. 2017).

Table 1
Compilation of Average N Isotopic Ratios in Meteorites and Other Rocky Bodies of the Solar System

Group	δ^{15}N (‰)	1σ
NC meteorites		
EH	−20.1	7.6
EL	−22.1	3.9
OC (H, L, LL)	−6.6	12.1
RC	−61.8	…
Ureilites	−23.7	26.0
Main group pallasites	−52.2	13.0
IC	−86.2	1.8
IIAB	−86.9	6.0
IIE	−4.1	2.7
IIIAB	−81.7	5.5
IIIE	−74.4	8.9
IVA	−28.9	5.2
IAB-MG	−60.6	5.2
CC meteorites		
CI	44.3	5.7
CM	25.6	18.7
CO	−4.1	6.9
CV	−17.0	5.9
CK	−28.4	1.6
CR	175.7	8.0
Tagish Lake	65.0	6.6
IIC	144.9	15.6
IID	10.0	3.5
IIF	10.8	5.2
IIIF	8.6	…
IVB	8.1	3.5
Rocky planets and the Moon		
Moon	5.0	…
Mars	−26.9	17.1
BSE	−1.5	1.5

Note. δ^{15}N (‰) values are the averages compiled from Table A1 and 1σ is 1 s.d. from the average. Data sources for δ^{15}N in Earth's mantle—(Grewal et al. 2021b), Mars' mantle—(Mathew & Marti 2001), and the Moon—(Mortimer et al. 2015).

Magmatic NC irons with accretion ages between ∼0.1 and 0.3 Ma after CAIs sample the earliest formed planetesimals in our solar system. The predicted accretion ages of nonmagmatic NC irons (IAB-MG and IIE) are later (∼1.4–1.5 Ma after CAIs), but their Hf–W ages were likely reset during impact-related events (Kruijer & Kleine 2019). CC irons are predicted to accrete ∼0.9–1 Ma after CAIs (Kruijer et al. 2017). However, accounting for poorly known parameters like the initial water/rock ratios in their parent bodies could push the accretion ages of CC irons to earlier timescales (Spitzer et al. 2021). The accretion ages of achondrites and chondrites have been estimated using thermal models based on ^{26}Al decay in combination with Al–Mg and Mn–Cr chronometers (Sugiura & Fujiya 2014). Despite the inherent uncertainties involved in the modeling of accretion ages, they are excellent tracers of the relative accretion ages of the parent bodies of chondrites and achondrites. The accretion ages of the parent bodies of ureilites are estimated to be similar to CC irons, i.e., ∼1 Ma after CAIs. Parent bodies of NC chondrites, i.e., ECs, OCs, and RCs, are predicted to have accreted ∼1.8–2.1 Ma after CAIs. The parent bodies of CC chondrites accreted rather late, with CO, CV, and CK chondrites accreting ∼2.6–2.7 Ma after CAIs and CM, CI, Tagish Lake, and CR chondrites accreting ∼3.5–3.85 Ma after CAIs.

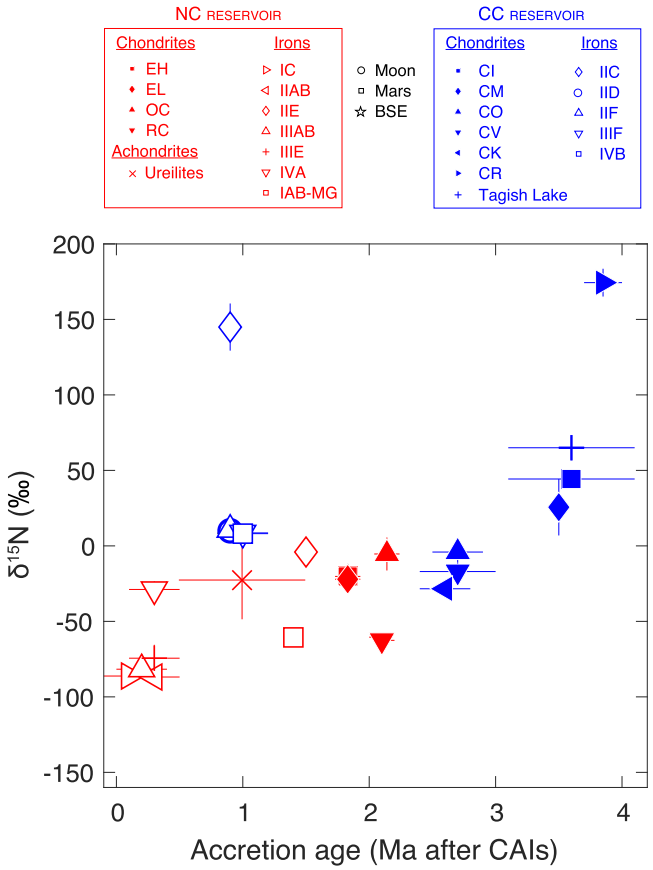

Figure 3. Nitrogen isotopic compositions of meteorites as a function of their accretion ages. δ^{15}N values of planetesimals (except IIE irons) accreting within ∼3 Ma after CAIs lie in a similar range followed by an increase for later accreting CM, CI, Tagish Lake, and CR chondrites. Note that the symbols of groups IID, IIF, IIIF, and IVB of CC iron meteorites are overprinted due to an overlap in their δ^{15}N values and accretion ages.

Even though δ^{15}N values can vary up to ∼50‰–70‰ for planetesimals accreting at similar timescales, a temporal trend exists between their δ^{15}N values and accretion ages (Figure 3). Importantly, both NC and CC meteorites follow this common trend. δ^{15}N values of meteorites whose parent bodies accreted within ∼3 Ma after CAIs—NC and CC irons, ureilites, NC chondrites (EC, OC, and RC), and early accreting CC chondrites (CV, CO, and CK)—lie in a similar range. δ^{15}N values of CC chondrites (CM, CI, Tagish Lake, and CR) sampling late accreting planetesimals are distinctly higher than all other classes of meteorites. Only IIC irons buck this common correlation of δ^{15}N values and accretion ages. This could either be due to the preferential retention of isotopically heavier N (akin to CR chondrites) during their differentiation or a result of the IIC iron parent body accreting materials that were isotopically distinct from both NC and CC reservoirs (Tornabene et al. 2020).

A common temporal trend in the δ^{15}N values of NC and CC meteorites indicates that planetesimals accreting at similar timescales irrespective of their growth zones exhibit similar N isotopic compositions. Importantly, CV, CO, and CK chondrites that have lower δ^{15}N values (lying in the range of NC meteorites) also have earlier accretion ages compared to other CC chondrites. Therefore, their N isotopic compositions cannot be explained by the accretion of materials during the purported late-stage mixing of NC and CC reservoirs. As samples from

contemporaneously accreting planetesimals exhibit similar δ^{15}N values irrespective of their growth zones, is it possible that planetesimals in the inner and outer disk were accreting isotopically similar N-bearing materials and the N isotopic compositions of meteorites simply reflect the effects of common, time-dependent parent body processing?

4. Effect of Parent Body Processing on Nitrogen Isotopic Compositions of Meteorites

The physical and chemical evolution of the interiors of early accreting planetesimals was controlled by a common parameter—heat released by the decay of short-lived radionuclides, primarily ^{26}Al. Planetesimals of comparable sizes accreting at different timescales accreted different amounts of ^{26}Al (Neumann et al. 2012). This led to them experiencing substantially different peak body temperatures resulting in varying exposure to thermal metamorphism (Hevey & Sanders 2006; Sahijpal et al. 2007). In addition, a temporal and spatial variation in the growth of meteorite parent bodies resulted in the accretion of materials with different water/rock ratios culminating in differential exposure to aqueous alteration (Lichtenberg et al. 2021). Therefore, planetesimals with the earliest accretion ages must have experienced the highest peak temperatures (assuming similar accretion rates and parent body sizes) and consequently undergone the largest extent of melting (Hevey & Sanders 2006; Neumann et al. 2012). This is reflected in the meteorite record with the parent bodies of differentiated meteorites (iron meteorites and stony achondrites) having accreted earlier relative to the parent bodies of chondrites. The interiors of planetesimals experienced higher temperatures than the surface layers resulting in undifferentiated crusts underlain by fully or partially differentiated mantles and cores (Hevey & Sanders 2006; Sahijpal et al. 2007; Neumann et al. 2012). The surface layers of the undifferentiated crusts are chondrite-like and the extent of thermal metamorphism in the surficial layers increases with depth (Elkins-Tanton et al. 2011). If the temporal trend in the N isotopic compositions of bulk meteorites is a direct result of the thermal evolution of their parent bodies (Figure 3), then this trend should also be observed in samples from different layers of a given planetesimal that experienced distinct peak temperatures. However, evidence for meteorites sampling multiple layers of a given planetesimal is presently lacking. Iron meteorites and achondrites retain the memory of late-stage, high-temperature igneous processes only (Neumann et al. 2012). Hence, they do not yield any information on the temperature-dependent evolution of the N isotopic compositions of their parent bodies. Chondritic samples with variable metamorphic indices, on the other hand, do capture the effects of parent body processing—thermal metamorphism and aqueous alteration—on the N abundances and isotopic compositions of surficial and/or sub-surficial layers within a given planetesimal (Alexander et al. 1998; Pearson et al. 2006). Importantly, the interiors of the parent bodies of iron meteorites and achondrites as well must have experienced temperatures akin to chondrites during their thermal evolution before heating to temperatures applicable for the onset of metal and silicate melting. Therefore, chondritic samples recording variable metamorphic indices are useful proxies to infer the effect of time-dependent thermal evolution on the N isotopic compositions of planetesimals.

Almost the entire N inventory of chondrites (except ECs) is hosted in organic matter. 70%–95% of organic matter is present in solvent/acid insoluble organic matter (IOM; comprising complex macromolecular material) and 5%–30% in solvent soluble organic matter (SOM; Alexander et al. 1998; Sephton et al. 2003; Alexander et al. 2007). In ECs, N is hosted in reduced refractory phases like osbornite (TiN), nierite (Si_3N_4), sinoite (Si_2N_2O), and as a substitute for O in the silicate network (Grady et al. 1986). However, relatively constant metamorphism-corrected nanodiamond abundances as a fraction of IOM in ECs, OCs, and CCs, and a release of ^{15}N-rich components during stepped combustion of ECs and OCs suggest that the parent bodies of all chondrites likely accreted CC-like precursor organics (Alexander et al. 1998, 2007, 2017). Organic matter is easily modified by heating at modest temperatures as well as on low- and high-temperature interactions with aqueous fluids (Sephton et al. 2003; Alexander et al. 2007). The effect of parent body processing, i.e., thermal metamorphism and aqueous alteration, on the primitive N inventories of planetesimals can be inferred by comparing their abundances in chondritic samples with variable metamorphic indices. A substantial drop in bulk N contents with increasing degrees of parent body processing has been reported within CCs, OCs, and ECs of varying petrologic grade (Hashizume & Sugiura 1995; Alexander et al. 1998; Pearson et al. 2006). This correlation of N abundances with metamorphic indices hints at a common mechanism controlling N loss as a function of the alteration of primitive organic matter (Alexander et al. 1998, 2007). In parallel, a gradual change in the N isotopic compositions with increasing degrees of thermal metamorphism and aqueous alteration has also been observed within chondritic groups (Alexander et al. 1998; Pearson et al. 2006; Alexander et al. 2007). For example, δ^{15}N values of unequilibrated OCs and CCs decrease with an increase in the degree of thermal metamorphism (Hashizume & Sugiura 1995; Pearson et al. 2006). A similar decrease in δ^{15}N values with an increasing degree of aqueous alteration has also been observed in CI, CM, and CR chondrites (Pearson et al. 2006). Experimental studies on hydrothermal alteration along with the stepwise combustion profiles of bulk chondrites and their isolated IOMs show a similar decrease in δ^{15}N values with increasing degrees of thermal metamorphism and aqueous alteration (Sephton et al. 2003; Foustoukos et al. 2021). Does the decrease of N contents and δ^{15}N values within a given chondrite group with increasing metamorphic indices indicate the common control of parent body processing on the evolution of N contents and isotopic compositions of planetesimals? To answer this, it is necessary to compare the N contents and δ^{15}N values of samples from different groups of chondrites across a common metamorphic index.

Thermal evolution of chondrites can be tracked by using their peak metamorphic temperatures ($T_{\rm eff}$), inferred via organic thermometry (Cody et al. 2008). As $T_{\rm eff}$ quantifies the effect of parent body metamorphism for individual samples from ECs, OCs, and CCs, it can be used to put different chondritic groups on a common petrological scale. This common scale is critical to ascertain if planetesimals in the inner and outer regions of the protosolar disk were affected by a universal process of N loss resulting in the variability of N isotopic compositions in meteorites. Figure 4(A) shows that N contents in bulk chondrites (which includes IOM residue, very fine-grained IOM that is either hard to recover or lost during treatment with acid solutions, SOM, and other inorganic N and C hosts; Table 2) display a sharp drop in their N inventories during thermal metamorphism. Importantly, low bulk N contents at high $T_{\rm eff}$ are displayed by chondritic samples from both NC and

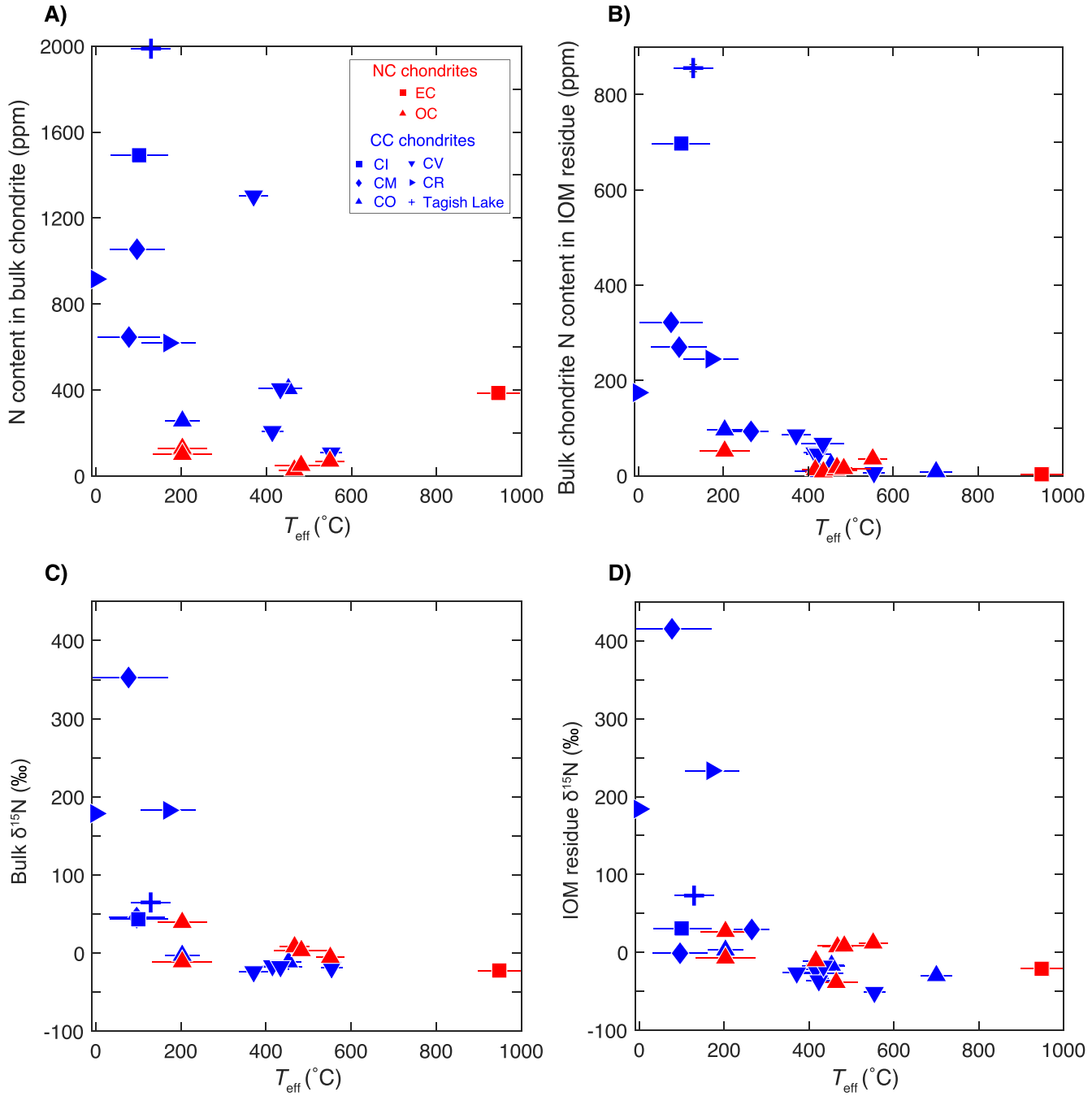

Figure 4. Nitrogen isotopic compositions of bulk chondrites and IOM residues compared with the effective temperatures (T_{eff}) of chondritic samples inferred from organic thermometry. Nitrogen contents as well as $\delta^{15}N$ values decrease sharply with an increasing degree of thermal metamorphism in planetesimals. The variation of N contents and $\delta^{15}N$ values at a given T_{eff} is likely a result of varying aqueous alteration. T_{eff} data is compiled from Cody et al. (2008). Refer to Table 2 for data compilation.

CC reservoirs. Relatively high bulk N in an EC sample at $T_{eff} \sim 950$ °C is related to the extremely reduced conditions during thermal metamorphism in its parent body resulting in the retention of N in reduced refractory phases (Grady et al. 1986). None of the parent bodies of other chondrites (as well as iron meteorites) experienced conditions as reduced as ECs (Righter et al. 2016). Therefore, retention of a substantial N inventory in the EC sample at high T_{eff} is related to the uniquely reduced conditions during thermal metamorphism in its parent body and must not be the norm. Analogous to bulk N contents, high losses with increasing T_{eff} are also recorded in the N contents of demineralized IOM residues of chondritic samples (left after treatment with CsF-HF solution; data compiled from Alexander et al. 2007, Table 2) (Figure 4(B)). Most of these chondrites also record effects of variable degrees of hydrothermal alteration resulting in the scatter of data at a given T_{eff} (Sephton et al. 2003; Foustoukos et al. 2021). However, unlike T_{eff}, there is no quantitative aqueous alteration index that can be applied across different groups of chondrites. CM chondrites—with well-defined aqueous alteration index—display a decrease in their N contents with an increasing degree of aqueous alteration (Figure 5(A)). A similar effect of aqueous alteration can result in the scatter of bulk N contents in CCs at $T_{eff} < \sim 200$°C (Figure 4(A)). T_{eff} of ECs, OCs, and CCs along

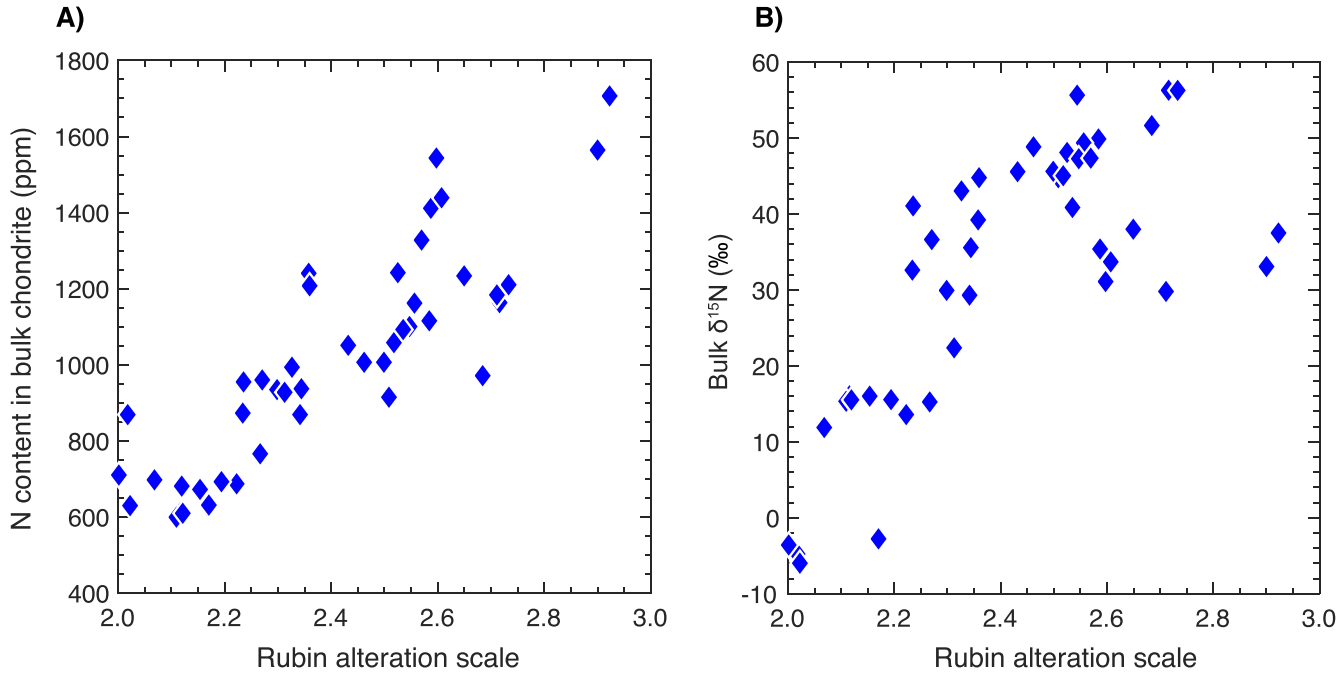

Figure 5. Nitrogen contents and isotopic compositions of CM chondrites as a function of their extent of aqueous alteration (here defined by the alteration scale from Rubin et al. 2007). Both N contents and δ^{15}N values decrease with increasing extent of aqueous alteration across CM chondrites. Note that the Bells chondrites are not plotted as their Rubin alteration scale index is currently lacking. CM chondrite data is compiled in Table A1 in the Appendix.

Table 2
Compilation of Peak Metamorphic Temperatures, N Abundances, and Isotopic Compositions of Chondritic Samples

Name	Group	$T_{\rm eff}$ (°C)	$T_{\rm eff}$ (1σ)	N Bulk (ppm)	N IOM (ppm)	δ^{15}N bulk (‰)	δ^{15}N IOM (‰)
EET 92042	CR2	0	0	912	176	178.7	184.1
GRO 95577	CR1	171	64	613	246	182.8	233.2
Bells	CM2	77	73	641	324	352.8	415.3
Murchison	CM2	96	65	1051	271	45.6	−1.0
Y86720	CM heated	265	42	…	95	…	29.5
Orgueil	CI1	101	68	1490	698	44.1	30.7
Tagish Lake	C2	129	46	1988	856	65.0	73.0
ALHA 77307	CO3.0	203	41	249	98	−2.7	3.0
Kainsaz	CO3.2/3.6	453	29	400	26	−11.1	−16.4
ALHA 77003	CO3.5	425	56	…	11	…	−27.1
Isna	CO3.7–3.8	700	37	…	10	…	−29.7
Kaba	CV3.1	371	34	1300	88	−23.7	−26.2
Vigarano	CV3.1/3.4	415	25	200	50	−15.9	−21.3
Mokoia	CV3.2/3.6	423	29	…	48	…	−36.3
Leoville	CV3.1/3.4	434	50	400	70	−17.1	−17.5
Allende	CV3.2/N3.6	554	25	100	9	−18.6	−51.2
Semarkona	LL3.0	203	58	121	54	39.3	26.9
MET 00452	LL3.05	203	70	93	0	−11.0	−7.2
Krymka	LL3.1	416	31	…	15	…	−10.7
WSG 95300	H3.3	464	50	…	14	…	−38.5
Tieschitz	H/L3.6	467	36	20	19	8.1	7.2
Chainpur	LL3.4	483	63	42	17	3.3	8.2
Bishunpur	LL3.15	551	34	61	37	−5.3	12.1
Indarch	EH4	948	50	380	5	−22.1	−20.9

Note. Data sources: $T_{\rm eff}$—(Cody et al. 2008); Bulk N content and δ^{15}N—(Pearson et al. 2006; Alexander et al. 2012); IOM N content and δ^{15}N—(Alexander et al. 2007).

with N contents and δ^{15}N values of bulk samples and their IOM residues are tabulated in Table 2.

δ^{15}N values of bulk chondrites as well as their IOM also drop sharply with increasing $T_{\rm eff}$ with no large positive δ^{15}N signatures at $T_{\rm eff} > \sim$200°C (Figures 4(C), (D)). This suggests a preferential loss of ^{15}N with increasing degree of thermal metamorphism. CR chondrites and Bells (CM) define the isotopically primitive end members whereas thermally altered CVs, COs, OCs, and ECs define the δ^{15}N values of evolved samples. Analogous to the variability of N contents at a given

T_{eff}, aqueous alteration likely causes the variation of $\delta^{15}N$ values in bulk chondrites and IOM. The effect of an increasing degree of aqueous alteration is shown to result in lower $\delta^{15}N$ values in CM chondrites (Figure 5(B)). Therefore, the sharp drop in $\delta^{15}N$ values from CR chondrites and Bells (CM)—with restricted water-rock interaction (Browning et al. 1996; Brearley 2006)—to aqueously altered Tagish Lake and CM chondrites could be a result of low-temperature interaction of aqueous fluids with primitive organics.

Figure 4 shows that parent body processing resulted in profound changes in the N abundances and isotopic compositions of planetesimals. A correlation of $\delta^{15}N$ values with T_{eff} across different groups of chondrites (Figures 4(C), (D)) as well as the intragroup variation of $\delta^{15}N$ values with aqueous alteration index (Figure 5(B)) suggests that (1) the organic matter was composed of several isotopically distinct N components, and 2) its relative stability was sensitive to parent body processing—thermal metamorphism and aqueous alteration. Using stepped combustion profiles of bulk chondrites, Sephton et al. (2003) suggested that the labile component of the organic matter is ^{15}N-rich, and the refractory component is ^{15}N-depleted. Similar observations have been made based on the stepped combustion profiles of isolated IOM by Alexander et al. (1998) and Sephton et al. (2003), i.e., IOM is composed of relatively labile ^{15}N-rich and refractory ^{15}N-depleted components. Therefore, the N isotopic composition of the more primitive chondrites must be controlled by the ^{15}N-rich components, with the contribution of the ^{15}N-poor components increasing with an increasing degree of parent body processing. The common correlation between N abundances and isotopic ratios of NC and CC chondrites with T_{eff} implies that their parent bodies accreted common organic precursors whose N isotopic compositions were affected by varying degrees of thermal metamorphism and/or aqueous alteration.

Is the effect of thermal metamorphism on $\delta^{15}N$ values of individual chondritic samples also reflected in the average $\delta^{15}N$ values of their parent bodies? As discussed earlier, the amount of thermal processing experienced by a planetesimal is primarily controlled by the amount of ^{26}Al accreted by it, and this amount is a direct reflection of its accretion age (assuming similar accretion rates and parent body sizes). Therefore, correlations between average $\delta^{15}N$ values and the accretion ages of chondrite parent bodies can be used to approximately estimate the effect of thermal processing on the N isotopic compositions of their surficial/sub-surficial layers. Figure 3 shows that the mean $\delta^{15}N$ values of chondrites follow a common correlation with the accretion ages of their parent bodies. The N isotopic compositions of chondrites with parent bodies having accretion ages of less than ~3 Ma after CAIs are ^{15}N-poor compared to those that accreted later. What is the cause behind this inflection of the N isotopic compositions of chondrites at ~3 Ma? The half-life of ^{26}Al decay is ~0.7 Myr. The surficial reservoirs of earlier accreting planetesimals (as sampled by thermally metamorphosed EC, OC, RC, CO, CV, and CK groups) must have been affected significantly by ^{26}Al decay-powered heating, resulting in the preferential loss of relatively labile ^{15}N-rich components. Whereas it is likely that parent bodies accreting ~3 Ma after CAIs did not undergo extensive heating due to the unavailability of adequate amounts of ^{26}Al. The parent bodies of CM, CI, Tagish Lake, and CR chondrites likely escaped the major heating effect of ^{26}Al decay, resulting in the preferential retention of relatively labile ^{15}N-rich components. An increase in the $\delta^{15}N$ values among these meteorites with increasing accretion ages was likely a result of low-temperature aqueous alteration powered by the heat released by the limited amounts of residual ^{26}Al within their parent bodies. Taken together, this combined evidence suggests that the parent bodies of all classes of chondrites—irrespective of their accretion ages and growth zones—accreted common organic precursors containing a mixture of labile and refractory components with higher and lower $^{15}N/^{14}N$ ratios, respectively. Therefore, N isotopic compositions exhibited by a chondrite sample directly reflect the effects of parent body processing on the planetesimal.

If NC and CC chondrites accreted common organic precursors, what about other classes of meteorites? Unlike chondrites, a common metamorphic index to evaluate the N isotopic compositions of other meteorite classes like iron meteorites is currently lacking. The N isotopic compositions of NC and CC iron meteorites (except the IIC group) follow the common correlation between $\delta^{15}N$ values and accretion ages exhibited by chondrites (Figure 3). $\delta^{15}N$ values of these groups of iron meteorites lie within the range of early accreting chondrite parent bodies. Therefore, akin to thermally metamorphosed EC, OC, RC, CO, CV, and CK groups, N in the iron meteorites was sourced from thermally evolved regions of the planetesimals which had preferentially lost relatively labile ^{15}N-rich components. Based on this evidence, it seems likely that the parent bodies of both NC and CC iron meteorites, akin to chondrite parent bodies, could have accreted common organic precursors. However, the $\delta^{15}N$ values of NC irons, especially the earliest accreting IC, IIAB, IIIAB, and IIIE groups, are distinctly lower than CC irons. This observation was used by Grewal et al. (2021b) to posit that the parent bodies of NC irons accreted N from a local source that was isotopically distinct from the outer solar system materials. Thermal processing of common organic precursors can provide an alternate explanation if the lower $\delta^{15}N$ values of NC irons relative to CC irons were simply a result of sampling bias, i.e., CC irons accreting as early as NC irons are missing from the meteorite record. Accordingly, the difference in the N isotopic compositions of NC-CC iron meteorites observed by Grewal et al. (2021b) might not reflect a true dichotomy in the N isotopic compositions of primitive organics in the NC and CC reservoirs.

5. Origin of Nitrogen in the Rocky Bodies of the Solar System

The findings of this study support an extremely early presence of organic precursors in the inner protosolar disk. As these organics likely had a presolar origin (Alexander et al. 1998, 2017), they must have retained their primordial characteristics by surviving extensive processing in the inner disk during the collapse of the molecular cloud. The presence of a ^{15}N-rich chondrite-like N in CAIs also suggests that organic precursors, or at least some of their components, escaped widespread nebular processing (Füri et al. 2015). These observations are contrary to the predictions based on the location of *soot/tar line,* which suggests that organics, including their refractory components, in the inner disk were destroyed within 1 Ma of solar system formation (Bermingham et al. 2020; Li et al. 2021). A widespread depletion of N in the inner solar system rocky protoplanets and planets despite the presence of organic precursors in the inner protosolar disk

attests to the importance of parent body processes like thermal metamorphism, aqueous alteration, core formation, and magma ocean degassing. A sharp drop in bulk N contents of chondrites at low degrees of metamorphism (Figure 4(A)) suggests that thermal metamorphism and aqueous alteration, contrary to high-temperature processes like core formation and magma ocean degassing (Grewal et al. 2019a, 2019b, 2020, 2021a), set the depletion of N in differentiated rocky bodies.

The starring role of parent body processes like thermal metamorphism and aqueous alteration in controlling the N abundances and isotopic compositions of planetesimals necessitates a fundamental reassessment of the utility of N isotopic ratios for tracing the source of life-essential volatiles in rocky planets. The findings of this study imply that planetesimals, independent of their growth zones and accretion ages, accreted common organic precursors and the N contents and isotopic ratios of meteorite samples record the extent of thermal and aqueous alteration experienced by their parent bodies. As these planetesimals underwent a time-dependent thermal evolution, different layers within a given planetesimal can exhibit a range of N isotopic ratios. For instance, surface layers of planetesimals would be more enriched in ^{15}N than the interiors as they experienced lower temperatures and consequently underwent a lower degree of thermal metamorphism. This suggests that the layers of the early accreting planetesimals experiencing the least parent body processing should record higher $^{15}N/^{14}N$ ratios, independent of their growth zone. Therefore, the N isotopic compositions recorded by a given group of meteorites do not represent the N composition of the entire parent body. More importantly, this also means that comparisons between N isotopic compositions of meteorites and rocky planets cannot be independently used to cosmolocate the source of volatiles. For instance, higher $^{15}N/^{14}N$ ratios in Earth's atmosphere relative to the mantle has been used as evidence for a dual origin of life-essential volatiles in the Earth, with the atmosphere acquiring N from the CC reservoir and the mantle from the NC reservoir (Piani et al. 2020; Grewal et al. 2021b). Mass balance calculations suggest that these reservoirs contributed almost equally to the N budget of the Earth (Piani et al. 2020; Grewal et al. 2021b). These conclusions rest on the assumption that δ^{15}N values of ECs/NC irons and CCs/CC irons represent the N isotopic compositions of NC and CC reservoirs, respectively. However, the findings of this study suggest that this assumption is not valid. δ^{15}N values of a given group of meteorites neither capture the N isotopic compositions of the entire planetesimal nor the N isotopic ratios of primitive reservoirs. Instead, they capture the cumulative effects of parent body processing on the primitive N present in different layers of their parent bodies. As a result, the source, i.e., NC or CC reservoir, of life-essential volatiles in rocky planets cannot be tracked by comparing their $^{15}N/^{14}N$ ratios (and potentially D/H and $^{13}C/^{12}C$ ratios) with those of meteorite samples. A better understanding of parent body processing and their role in determining the N, C, and H isotopic compositions of multiple layers of planetesimals as a function of their growth zones and accretion ages is needed to infer the timing and source of life-essential volatiles in the rocky planets of our solar system.

6. Conclusions

In this study, I used the N isotopic compositions of meteorites as a function of their growth zones and accretion ages to infer whether planetesimals in the NC and CC reservoirs accreted isotopically heterogeneous precursors or not. A comparison of $^{15}N/^{14}N$ ratios with the isotopically anomalies of Ti, Cr, and Mo in chondrites, achondrites, and iron meteorites suggests that though NC meteorites generally have lower $^{15}N/^{14}N$ ratios than CC meteorites, there is an overlap in their N isotopic compositions. Therefore, unlike iron meteorites, the combined meteorite record does not suggest an isotopic dichotomy in the N isotopic compositions of NC and CC reservoirs. A comparison between the $^{15}N/^{14}N$ ratios of meteorites and the accretion ages of their parent bodies suggests that this overlap cannot be explained by the late-stage mixing of NC and CC reservoir-derived materials. As the $^{15}N/^{14}N$ ratios of meteorites (except for IIC irons, Bells-CM, CB, and CH chondrites with anomalous N isotopic compositions requiring the role of currently unknown additional processes), follow a common correlation with their accretion ages, N isotopic compositions exhibited by meteorites must be a direct reflection of a common time-dependent process in inner and outer solar system planetesimals—namely their thermal evolution as a function of heating caused by ^{26}Al decay. N abundances and isotopic ratios in chondritic samples from NC and CC reservoirs follow a common correlation with their peak metamorphic temperatures. This correlation can be best explained if the planetesimals independent of their growth zones and accretion ages accreted common organic precursors which contained a mixture of labile and refractory components with higher and lower $^{15}N/^{14}N$ ratios, respectively. Due to the differential stability of these components, the N isotopic compositions within and among planetesimals could show large degrees of variations depending upon the extent of parent body processing experienced by the planetesimals. As a result, the heterogeneity of N isotopic compositions of meteorites does not reflect heterogeneity in the N isotopic compositions of primordial reservoirs but alludes to the differential effects of parent body processing. In light of this evidence, it can be concluded that the contribution of inner and outer solar system reservoirs to the present-day rocky planets cannot be constrained by the isotopic ratios of N, and potentially other volatiles like C and H, in meteorites.

Amrita P. Vyas is thanked for helping improve communication. Constructive comments by two anonymous reviewers are greatly appreciated. This work was supported by a Barr Foundation Postdoctoral Fellowship from the California Institute of Technology.

Appendix

The appendix comprises of Table A1 where the N isotopic compositions of individual samples of chondrites and ureilites are tabulated.

Table A1
Compilation of N Isotopic Compositions of Chondrites and Ureilites

Groups	Name	δ^{15}N (‰)	Groups	Name	δ^{15}N (‰)
CM2	ALHA 81002 H	13.6	CO3	MIL 05013	−7.2
CM1/2	ALH 83100 H	11.9	CO3	DOM 08006	6.5
CM2	ALH 84029	15.5	CO3	DOM 03238	−6.0
CM2	ALH 84034	16.1	CO3	DOM 08004	−7.9
CM2	ALH 84042	15.3	CO3	DOM 08006 II	8.6
CM2	ALH 84044	15.3	CO3	DOM 10104	−5.9
CM2	ALH 85013	32.6	CO3	MIL 03377	−5.5
CM2	Banten	44.8	CO3	MIL 03442	−8.5
CM2	Cold Bokkeveld H	16.0	CO3	MIL 05013 II	−4.0
CM2	DNG 06004	49.9	CO3	MIL 05024	−7.8
CM2	DOM 08003	41.1	CO3	MIL 07182	−8.5
CM2	DOM 08013	56.3	CO3	MIL 07193	−8.4
CM2	EET 96006	39.2	CO3	MIL 07709	−8.1
CM2	EET 96016	44.8	CO3	MIL 090010	−4.9
CM2	GRA 98074	49.4	CO3	MIL 090038	−3.3
CM2	GRO 95566	55.7	CO3/CM(H)?	MIL 090073	10.5
CM2	LAP 02239	45.6	CO3	MIL 090785	13.9
CM2	LAP 02333	35.4	CO3	Kainsaz	−11.1
CM2	LAP 02336	33.7	CO3	Felix	−8.8
CM2	LAP 03718	31.1	CO3	Ornans	−10.5
CM2	LAP 03785	36.6	CO3	Lancé	−7.4
CM2	LEW 85311	33.1	CO3	Warrenton	−6.8
CM2	LEW 85312	37.5	CK4	Karoonda	−28.4
CM2	LEW 87016	48.1	EH4	Abee	−29.2
CM2	LEW 87022	29.9	EH4	Indarch	−22.1
CM2	LEW 87148	43.0	EH4	Kota-Kota	−19.7
CM2	LEW 88001	48.8	EH4	Kota-Kota	−19.7
CM2	LEW 90500	35.6	EH4	South Oman	−27.4
CM2	LON 94102	38.0	EH4	South Oman	−16.6
CM2	MAC 88101	51.6	EH5	St. Mark's	−6.3
CM2	MAC 88176	22.4	EL6	Atlanta	−24.9
CM2	MCY 05230	47.3	EL6	Daniel's Kuil	−15.2
CM2	MET 00432	29.8	EL6	Khairpur	−24.3
CM1	MET 01070 H	−4.8	EL6	N.W. Forrest	−23.4
CM2	Mighei H	29.3	EL6	Yilmia	−22.7
CM2	Murchison	45.6	H3.9/4	ALHA 78084	−1.0
CM2	Murray H	45.0	H3.7	Grady 1937	16.8
CM2	Nagoya II	15.5	H3	Y791500	−15.0
CM2	Nogoya H	15.6	H3	Y82038	−2.9
CM2	QUE 97990 H	40.9	LL3.4/3.7	Mezo Madaras	8.3
CM2	QUE 99355	15.3	L3.8	Y74024	−10.8
CM2	SCO 06014	−2.8	LL3.4	Chainpur	3.9
CM1	SCO 06043 H	−3.6	H3.5	Allan Hills A81024	−4.7
CM1	SCO 06043 II	−6.0	H3.7	Alan Hills A77299	−4.4
CM2	TIL 91722	56.3	L3	Allan Hills A77167	−18.1
CM2	Y 791198 H	47.4	LL3.4	Chainpur	−15.7
CM2	Cold Bokkeveld	27.0	L3.3	Elephant Moraine 83399	5.1
CM2	Nogoya	21.1	LL3.4/3.7	Meso Madaras-a	12.6
CM2	Mighei	28.3	LL3.4/3.7	Meso Madaras-a	−4.1
CM2	Murray	48.0	L3.5	Allan Hills A78119	4.5
CM2	Murchison	52.7	H3.2/3.4	Allan Hills A81251-a	−18.7
CM2	Erakot	15.7	H3.2/3.4	Allan Hills A81251-b	−10.6
CM2	Kivesvaara	19.9	H3.2/3.4	Allan Hills A81251-c	−26.2
CM2	Bells (C)	352.8	H3.2/3.4	Allan Hills A81251-d	−39.2
CM2	Bells (W)	359.7	L3.1/3.3	Allan Hills 83010	−7.3
CR2	Al Rais	160.6	L3.2/3.5	Allan Hills 83007-a	−7.1
CR2	EET92042	178.7	L3.2/3.5	Allan Hills 83007-b	−4.4
CR2	EET 96286	173.0	L3.1	Lewis Cliff 86022	−8.6
CR2	GRA 95229	178.2	L3	Allan Hills 78046	−11.2
CR1	GRO95577	182.8	L3.7	Allan Hills 90411	−6.0
CR2	LAP 02342	162.8	RC	PCA 91002	−61.8
CR2	LAP 04720	166.1	Ureilites	AS 7	−48.2
CR2	MET 00426	179.8	Ureilites	AS 22	−29.4
CR2	PCA 91082	177.1	Ureilites	AS 27	−7.5

Table A1
(Continued)

Groups	Name	δ^{15}N (‰)	Groups	Name	δ^{15}N (‰)
CR2	QUE 99177	184.1	Ureilites	AS 36	−24.1
CR2	Renazzo	173.9	Ureilites	AS 44	−52.1
CR2	MIL 090657	182.9	Ureilites	ALHA 77257-50	−3.6
CR2	MIL 090657 II	184.2	Ureilites	Dyalpur	−3.2
CI1	Orgueil BM	44.1	Ureilites	Goalpara	0.2
CI1	Orgueil Smith.	35.9	Ureilites	Kenna	−24.8
CI1	Ivuna	44.9	Ureilites	North Haig	26.2
CI1	Orgueil	44.6	Ureilites	Havero	−4.4
CI1	Alais	52.0	Ureilites	ALH81101	−8.6
Tagish Lake	TL 11i	59.7	Ureilites	Kenna	−70.4
Tagish Lake	TL 11h	62.6	Ureilites	Lahrauli	−2.3
Tagish Lake	TL 5b	76.2	Ureilites	LEW85328	−25.1
Tagish Lake	Tagish Lake	61.5	Ureilites	ALH82130	−10.7
CV3	Kaba	−23.7	Ureilites	ALH78019	−13.5
CV	LAR 06317	−25.0	Ureilites	Nilpena	−37.6
CV3?	QUE 99038	−8.6	Ureilites	ALHA 77257-1	−53.7
CV3	Kaba	−9.2	Ureilites	ALHA 77257-2	−27.7
CV3	Vigarano	−15.9	Ureilites	ALHA 77257-3	−4.1
CV3	Grosnaja	−18.0	Ureilites	A-881931-1	−18.3
CV3	Allende	−18.6	Ureilites	A-881931-2	−1.6
CV3	Leoville	−17.1	Ureilites	Y-791538	−69.3
CO3	ALH 77307	−2.7	Ureilites	Y-790981	−78.7

Note. Data sources: CM, CR, CI, Tagish Lake, CV—(Pearson et al. 2006; Alexander et al. 2012); CO—(Pearson et al. 2006; Alexander et al. 2018); CK—(Pearson et al. 2006); EC—(Grady et al. 1986); OC—(Hashizume & Sugiura 1995; Sugiura et al. 1998); RC—(Sugiura & Zashu 1995); Ureilites—(Grady et al. 1985; Yamamoto & Hashizume 1998; Rai et al. 2003; Downes et al. 2015).

ORCID iDs

Damanveer S. Grewal https://orcid.org/0000-0002-5653-1543

References

Abernethy, F. A. J., Verchovsky, A. B., Franchi, I. A., & Grady, M. M. 2018, M&PS, 53, 375
Abernethy, F. A. J., Verchovsky, A. B., Starkey, N. A., et al. 2013, M&PS, 48, 1590
Alexander, C. M. O., Bowden, R., Fogel, M. L., et al. 2012, Sci, 337, 721
Alexander, C. M. O., Cody, G. D., de Gregorio, B. T., Nittler, L. R., & Stroud, R. M. 2017, ChEG, 77, 227
Alexander, C. M. O., Greenwood, R. C., Bowden, R., et al. 2018, GeCoA, 221, 406
Alexander, C. M. O., Russell, S. S., Arden, J. W., et al. 1998, M&PS, 33, 603
Alexander, C. M. O. D., Fogel, M., Yabuta, H., & Cody, G. D. 2007, GeCoA, 71, 4380
Bermingham, K. R., Füri, E., Lodders, K., & Marty, B. 2020, SSRv, 216, 133
Brearley, A. J. 2006, in Meteorites and the Early Solar System II, ed. D. S. Lauretta & H. Y. McSween, Jr. (Tucson, AZ: Univ. Arizona Press), 587
Browning, L. B., McSween, H. Y., & Zolensky, M. E. 1996, GeCoA, 60, 2621
Budde, G., Burkhardt, C., & Kleine, T. 2019, NatAs, 3, 736
Cody, G. D., Alexander, C. M. O., Yabuta, H., et al. 2008, E&PSL, 272, 446
Dasgupta, R., & Grewal, D. S. 2019, in Deep Carbon: Past to Present, ed. B. Orcutt, I. Daniel, & R. Dasgupta (Cambridge: Cambridge Univ. Press), 4
Downes, H., Abernethy, F. A. J., Smith, C. L., et al. 2015, M&PS, 50, 255
Elkins-Tanton, L. T., Weiss, B. P., & Zuber, M. T. 2011, E&PSL, 305, 1
Foustoukos, D. I., Alexander, D., & Cody, G. D. 2021, GeCoA, 300, 44
Franchi, I. A., Wright, I. P., & Pillinger, C. T. 1993, GeCoA, 57, 3105
Füri, E., Chaussidon, M., & Marty, B. 2015, GeCoA, 153, 183
Füri, E., & Marty, B. 2015, NatGe, 8, 515
Grady, M. M., Wright, I. P., Carr, L. P., & Pillinger, C. T. 1986, GeCoA, 50, 2799
Grady, M. M., Wright, I. P., Swart, P. K., & Pillinger, C. T. 1985, GeCoA, 49, 903
Grewal, D. S., Dasgupta, R., & Farnell, A. 2020, GeCoA, 280, 281
Grewal, D. S., Dasgupta, R., Holmes, A. K., et al. 2019a, GeCoA, 251, 87
Grewal, D. S., Dasgupta, R., Hough, T., & Farnell, A. 2021a, NatGe, 14, 369
Grewal, D. S., Dasgupta, R., & Marty, B. 2021b, NatAs, 5, 356
Grewal, D. S., Dasgupta, R., Sun, C., Tsuno, K., & Costin, G. 2019b, SciA, 5, eaau3669
Hashizume, K., & Sugiura, N. 1995, GeCoA, 59, 4057
Hevey, P. J., & Sanders, I. S. 2006, M&PS, 41, 95
Javoy, M. 1997, GeoRL, 24, 177
Keil, K. 2010, ChEG, 70, 295
Keil, K. 2012, ChEG, 72, 191
Kleine, T., Budde, G., Burkhardt, C., et al. 2020, SSRv, 216, 55
Krot, A. N., Amelin, Y., Bland, P., et al. 2009, GeCoA, 73, 4963
Kruijer, T. S., Burkhardt, C., Budde, G., & Kleine, T. 2017, PNAS, 114, 6712
Kruijer, T. S., & Kleine, T. 2019, GeCoA, 262, 92
Kruijer, T. S., Touboul, M., Fischer-Godde, M., et al. 2014, Sci, 344, 1150
Li, J., Bergin, E. A., Blake, G. A., Ciesla, F. J., & Hirschmann, M. M. 2021, SciA, 7, eabd3632
Lichtenberg, T., Drążkowska, J., Schönbächler, M., Golabek, G. J., & Hands, T. O. 2021, Sci, 371, 365
Marty, B. 2012, E&PSL, 313-314, 56
Marty, B., Chaussidon, M., Wiens, R. C., Jurewicz, A. J. G., & Burnett, D. S. 2011, Sci, 332, 1533
Mathew, K. J., & Marti, K. 2001, JGR, 106, 1401
Mittlefehldt, D. W. 2002, M&PS, 37, 703
Mortimer, J., Verchovsky, A. B., Anand, M., Gilmour, I., & Pillinger, C. T. 2015, Icar, 255, 3
Neumann, W., Breuer, D., & Spohn, T. 2012, A&A, 543, A141
Pearson, V. K., Sephton, M. A., Franchi, I. A., Gibson, J. M., & Gilmour, I. 2006, M&PS, 41, 1899
Piani, L., Marrocchi, Y., Rigaudier, T., et al. 2020, Sci, 369, 1110
Prombo, C. A., & Clayton, R. N. 1993, GeCoA, 57, 3749
Rai, V. K., Murty, S. V. S., & Ott, U. 2003, GeCoA, 67, 2213
Righter, K., Sutton, S. R., Danielson, L., Pando, K., & Newville, M. 2016, AmMin, 101, 1928
Rubin, A. E., Trigo-Rodríguez, J. M., Huber, H., & Wasson, J. T. 2007, GeCoA, 71, 2361
Sahijpal, S., Soni, P., & Gupta, G. 2007, M&PS, 42, 1529

Sephton, M. A., Verchovsky, A. B., Bland, P. A., et al. 2003, GeCoA, 67, 2093
Spitzer, F., Burkhardt, C., Budde, G., et al. 2020, ApJL, 898, L2
Spitzer, F., Burkhardt, C., Nimmo, F., & Kleine, T. 2021, E&PSL, 576, 117211
Sugiura, N., & Fujiya, W. 2014, M&PS, 49, 772
Sugiura, N., & Hashizume, K. 1992, E&PSL, 111, 441
Sugiura, N., Kiyota, K., & Hashizume, K. 1998, M&PS, 33, 463
Sugiura, N., & Zashu, S. 1995, in Proc. NIPR Symp. 8, Nineteenth Symp. on Antarctic Meteorites, ed. K. Yanai (Tokyo: National Institute of Polar Research), 273
Tornabene, H. A., Hilton, C. D., Bermingham, K. R., Ash, R. D., & Walker, R. J. 2020, GeCoA, 288, 36
Warren, P. H. 2011, E&PSL, 311, 93
Yamamoto, T., & Hashizume, K. O. 1998, M&PS, 33, 857